

Interaction of Surfactants and Polyelectrolyte-Coated Liquid Crystal Droplets

Tanmay Bera, Jiyu Fang

Department of Materials Science and Engineering, University of Central Florida, Orlando, USA
Email: Jiyu.Fang@ucf.edu

Received 17 August 2014; revised 11 September 2014; accepted 2 October 2014

Copyright © 2014 by authors and Scientific Research Publishing Inc.
This work is licensed under the Creative Commons Attribution International License (CC BY).
<http://creativecommons.org/licenses/by/4.0/>



Open Access

Abstract

It is known that the adsorption of surfactants at the liquid crystal (LC)/aqueous interface can induce a bipolar-to-radial director configuration of LC droplets dispersed in aqueous solution. In this paper, we study the effect of charged polyelectrolyte-coating on the interaction of surfactants and LC droplet cores by observing the director configuration of the LC droplet cores as a function of surfactant concentrations. It is found that surfactants can penetrate into the polyelectrolyte coating and react with the LC droplet cores to induce the bipolar-to-radial transition of the LC inside the droplet cores. However, the concentration of charged surfactants required to induce the configuration transition of the LC droplet cores is affected by the charged polyelectrolyte coating. The effect is significantly enlarged with decreasing the alkyl chain length of charged surfactants. Our results highlight the possibility of engineering polyelectrolyte coatings to tune the interaction of LC droplets with analysts, which is critical towards designing LC droplet based sensors.

Keywords

Liquid Crystals, Droplets, Polyelectrolyte Coatings, Surfactants, Configuration Transitions

1. Introduction

Liquid crystal (LC) droplets dispersed in aqueous solution are an interesting stimuli-responsive material [1]. They have been used as a model system for studying particle rotations [2] [3], optical momentum transfers [4], and optical vortex generations [5]. In recent years, LC droplets have also emerged as a unique optical probe for the detection of chemical and biological species and their reactions at the surface of the droplets [6]. The director configuration of LC droplets is known to reflect the balance between the elasticity and the surface anchoring of

the LC inside the droplets. Thus, the adsorption of chemical and biological species at the LC/aqueous interface may disrupt the balance to trigger the configuration transition of the LC inside the droplets, which can be easily observed with a polarizing optical microscope. The ultra-sensitivity of naked LC droplets has been proven in sensing bacterial endotoxin in aqueous solution [7]. However, naked LC droplets in aqueous solution are unstable and tend to coalesce over time. There has been interest in stabilizing and functionalizing LC droplets in aqueous solution by the adsorption of polymers at the LC/aqueous interface for sensor applications [8]-[20]. It has been shown that the adsorption of polyelectrolytes at the LC/aqueous interface can stabilize the LC droplets in aqueous solution [10] [13] [14]. Polyelectrolyte-coated LC droplets can be further modified by the adsorption of oppositely charged polyelectrolytes. It has been shown that the multilayer coating formed by the layer-by-layer adsorption of negatively charged poly(styrenesulfonate sodium) (PSS) and positively charged poly(allylamine hydrochloride) (PAH) is permeable for surfactants [10]. The permeated surfactants are able to react with the LC droplet cores and induce the bipolar-to-radial configuration transition of the LC inside the droplet cores. However, the PSS/PAH multilayer coating is found to reduce the response time of the LC droplet cores to surfactants by two orders of magnitude compared with naked LC droplets dispersed in aqueous solution.

In this paper, we coat 4-*n*-pentyl-4'-cyanobiphenyl (5CB) droplets with a bipolar configuration by the adsorption of both positively and negatively charged polyelectrolytes at the 5CB/aqueous interface to study the influence of polyelectrolyte coatings on the interaction of surfactants with the 5CB droplet cores by observing their configuration transitions as a function of surfactant concentrations. Polyelectrolytes used in our experiments are positively charged chitosan (CHT) and negatively charged polystyrene sulfonate (PSS). Surfactants used in our experiments are anionic sodium alkyl sulfate (SC_nS , $n = 18, 16, 14,$ and 12), cationic alkyl trimethylammonium bromide (C_nTAB , $n = 18, 16, 14,$ and 12) and nonionic tetraethylene glycol alkyl ether (C_nE_4 , $n = 14$ and 12). Although these surfactants are able to penetrate into the polyelectrolyte coatings to induce the bipolar-to-radial transition of the LC droplet cores, the concentration of charged surfactants required to induce the bipolar-to-radial configuration transition of the 5CB droplet cores is affected by charged polyelectrolyte coating. The effect of charged polyelectrolyte coatings is significantly enlarged with the decrease of the alkyl chain length of charged surfactants.

2. Experimental Section

2.1. Materials

Chitosan (CHT, $M_w \sim 190$ kDa), polystyrene sulfonate (PSS, $M_w \sim 70$ kDa), sodium alkyl sulfate (SC_nS , $n = 18, 16, 14,$ and 12 , 99% purity), alkyl trimethylammonium bromide (C_nTAB , $n = 18, 16, 14,$ and 12 , 99% purity) and tetraethylene glycol alkyl ether (C_nE_4 , $n = 14$ and 12 , 99% purity) were purchased from Sigma-Aldrich. Liquid crystals used in our experiments were 4-*n*-pentyl-4'-cyanobiphenyl (5CB, 98% purity) from Sigma-Aldrich. It shows a nematic phase in the temperature range from 23.5°C to 35.3°C . All chemicals were used without further purification. Water used in our experiments was purified with using Easypure II system (18.2 M Ω cm and pH 5.4).

2.2. Experimental Methods

Polyelectrolyte-coated 5CB droplets were formed by mixing 100 μL 5CB, 100 mL deionized water, and 100 mg polyelectrolytes with a sonicator for 15 min. The 5CB droplets were then purified through centrifugation to remove excess polyelectrolytes. The purified 5CB droplets were analyzed with an optical microscope to estimate their concentrations, in which a drop (2 μL) of 5CB droplet solution was placed between two cover glass slides and a large number of optical microscopy images were captured to represent the whole sample area. The number of the 5CB droplets confined by the two cover glass slides was carefully counted from the optical microscopy images and then used to calculate their concentrations in the initial solution. The final concentration of polyelectrolyte-coated 5CB droplets was adjusted to $\sim 8.2 \times 10^8$ droplets per mL for all experiments. Surfactant solution with desired concentrations was prepared by dissolving surfactants into deionized water and then mixed with polyelectrolyte-coated 5CB droplets.

2.3. Characterizations

The director configuration of the 5CB inside the droplets was analyzed with a polarized optical microscope

(Olympus BX40) in transmission mode. A large number of polarized optical microscopy images of 5CB droplets was captured and then analyzed to estimate the percentage of the 5CB droplets, which underwent the director configuration transition after being exposed to surfactant solution for 30 min. ζ -potential measurements were carried out using Zetasizer Nano ZS90 (Malvern Instruments Inc.) at room temperature under a cell-driven voltage of 30 V, in which 750 μL of polyelectrolyte-coated 5CB droplet solution was added into the zeta potential cuvettes and the average of 10 scans was taken for each measurements. The size of polyelectrolyte-coated 5CB droplets in aqueous solution was measured with dynamic light scattering (PD 2000DLS).

3. Results and Discussion

The chemical structures of CHT, PSS, SC_nS , C_nTAB , and C_nE_4 are shown in **Figure 1**. 5CB droplets were formed in deionized water with positively charged CHT or negatively charged PSS at pH 5.4. The adsorption of these charged polyelectrolytes at the 5CB/water interface is evident from ζ -potential measurements. The ζ -potentials of CHT and PSS-coated 5CB droplets are +38 mV and -43 mV, respectively. The average diameter of CHT and PSS-coated 5CB droplets is $\sim 0.70 \pm 0.15 \mu\text{m}$. **Figure 2(a)** shows a polarizing optical microscopy image of positively charged CHT-coated 5CB droplets in water. The CHT-coated 5CB droplets are stable and show a bipolar configuration, suggesting a parallel surface anchoring of the 5CB in the droplet cores. After being incubated with negatively charged SC_{12}S in water for 30 min, the CHT-coated 5CB droplets gradually transit into a radial

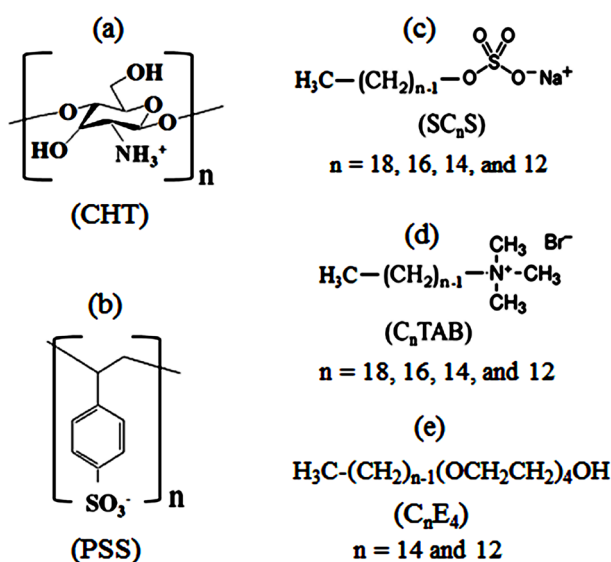


Figure 1. (a) Chemical structure chitosan (CHT); (b) polystyrene sulfonate (PSS); (c) sodium alkyl sulfonate (SC_nS); (d) alkyl trimethylammonium bromide (C_nTAB); (e) tetraethylene glycol alkyl ether (C_nE_4).

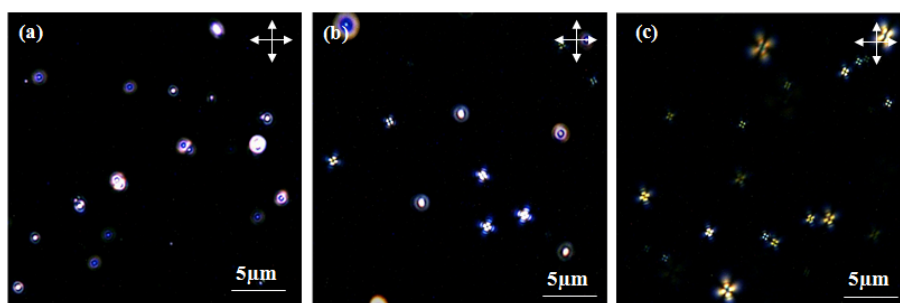


Figure 2. Polarizing optical microscopy images of CHT-coated 5CB droplets in water containing: (a) 0.0 μM ; (b) 25 μM ; (c) 50 μM SC_{12}S . The direction of the polarizer and analyzer is indicated by white arrows.

configuration (**Figure 2(b)** and **Figure 2(c)**), suggesting a perpendicular anchoring of the 5CB in the droplet cores. In addition, we note that the ζ -potentials of CHT-coated 5CB droplets drop from +38 mV to +12 mV after 30 min incubation with negatively charged SC₁₂S. It has been shown that the adsorption of SC₁₂S at the surface of naked 5CB droplets dispersed in water can induce the bipolar-to-radial configuration transition of naked 5CB droplets [21] [22]. Thus, we can conclude that negatively charged SC₁₂S penetrates into the positively charged CHT coating and react with the 5CB droplet cores, inducing the bipolar-to-radial transition shown in **Figure 2**. It is also visible from **Figure 2(b)** that the bipolar-to-radial transition of small CHT-coated 5CB droplets is faster than large CHT-coated 5CB droplets.

Figure 3(a) shows the transition curves of positively charged CHT-coated 5CB droplets as a function of SC_nS concentrations, in which the total number of the droplets is kept the same ($\sim 8.2 \times 10^8 \text{ mL}^{-1}$). For $n = 12$, the bipolar-to-radial configuration transition of CHT-coated 5CB droplets starts at the SC₁₂S concentration of $\sim 14 \mu\text{M}$. All the CHT-coated 5CB droplets transit into the radial configuration when the concentration of SC₁₂S reaches to $\sim 28 \mu\text{M}$. The transition curves of CHT-coated 5CB droplets gradually shift to left with the increase of n (**Figure 3(a)**). For $n = 18$, the 100% transition of CHT-coated 5CB droplets occurs at the SC₁₈S concentration of $\sim 4 \mu\text{M}$, which is seven times lower than the SC₁₂S concentration ($\sim 28 \mu\text{M}$) required to induce the 100% transition of CHT-coated 5CB droplets. These concentrations are significantly lower than the critical micelle concentration of SC₁₂S (7 mM) and SC₁₈S (0.1 mM), suggesting that no aggregation occurs for SC₁₂S and SC₁₈S, which were used in our experiments. The chain length-dependent transition should be related to the anchoring energy of SC_nS, which increases with the increase of its alkyl chain lengths [23]. Thus, we can expect that CHT-coated 5CB droplets are more susceptible to SC_nS with longer alkyl chain lengths, which explain why the concentration of SC_nS required inducing the bipolar-to-radial transition of CHT-coated 5CB droplets decreases with the increase of SC_nS chain lengths. **Figure 3(b)** shows that the transition curves of negatively charged PSS-coated 5CB droplets as a function of SC_nS concentrations, in which the total number of the droplets remains the same ($\sim 8.2 \times 10^8 \text{ mL}^{-1}$). The transition curves gradually shift to left with the increase of n , which is similar to the positively charged CHT-coated droplets. However, the concentration of negatively charged SC_nS required to induce the bipolar-to-radial transition of negatively charged PSS-coated 5CB droplets is larger than that of negatively charged CHT-coated 5CB droplets. This is a result of the reduced penetration of negatively charged SC_nS into the negatively charged PSS-coated 5CB droplets due to electrostatic repulsion because the anchoring energy depends on the density of the SC_nS adsorbed at the surface of 5CB droplets. It has been shown that the density increase of surfactant layers favors the planar-to-perpendicular anchoring transition of LCs [24]-[26]. For the comparison, we plot the SC_nS concentration required to induce the 100% transition of CHT- and PSS-coated 5CB droplets as a function of n (**Figure 3(c)**). It is clear from **Figure 3(c)** that the difference is enlarged with the decrease of n . The concentration of SC₁₈S required to induce the 100% transition of CHT- and PSS-coated 5CB droplets is $4 \mu\text{M}$ and $12 \mu\text{M}$, respectively. While the concentration of SC₁₂S required inducing the 100% transition of CHT- and PSS-coated 5CB droplets is $28 \mu\text{M}$ and $200 \mu\text{M}$, respectively. This result suggests that the polyelectrolyte coating has more significant impact for the interaction between the 5CB droplet cores and the

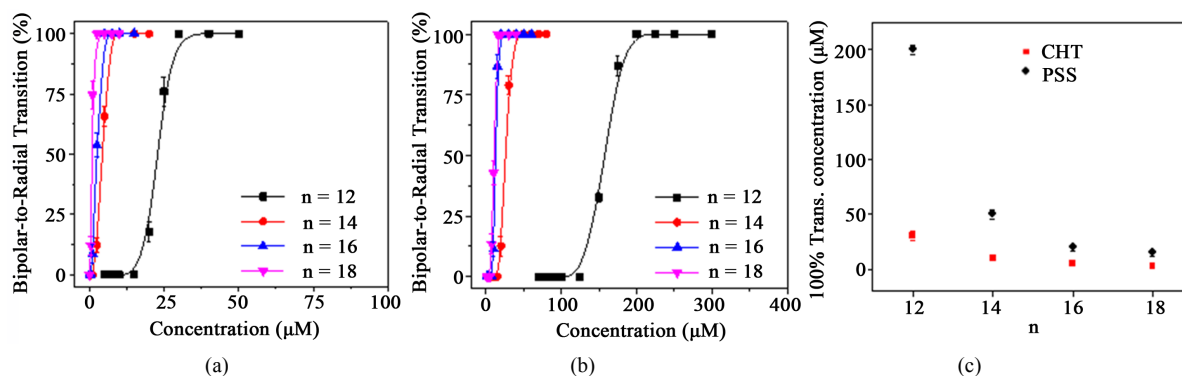


Figure 3. (a) The bipolar-to-radial transition percentage of CHT-coated 5CB droplets as a function of SC_nS concentrations; (b) The bipolar-to-radial transition percentage of PSS-coated 5CB droplets as a function of SC_nS concentrations; (c) SC_nS concentration required to induce the 100% transition of CHT- and PSS-coated 5CB droplets as a function of n . The data points shown in 3(a) and 3(b) were obtained from the statistical results of 100 droplets from each sample.

SC_nS with shorter alkyl chain lengths. The negatively charged head group of SC_nS is expected to locate at the outside of the negatively charged PSS coating due to electrostatic repulsion. The extent of the penetrated alkyl chain of SC_nS into the 5CB droplet cores decreases with the decrease of their lengths. Thus, the effect of the PSS coating increases with the decrease of the alkyl chain length of SC_nS.

It has shown that the adsorption of alkyl trimethylammonium bromide (C_nTAB) with $n = 18, 16, 14,$ and 12 at the LC/aqueous interface can also induce the bipolar-to-radial director configuration transition of naked LC droplets [22]. The chain length-dependent transition is also observed for CHI- and PSS-coated 5CB droplets after being exposed to positively charged C_nTAB. **Figure 4(a)** shows the transition curves of CHT-coated 5CB droplets from the bipolar to the radial configuration as a function of C_nTAB concentrations, in which the total number of the droplets is kept the same ($\sim 8.2 \times 10^8 \text{ mL}^{-1}$). For $n = 12$, the configuration transition of CHT-coated 5CB droplets starts at the C₁₂TAB concentration of $200 \mu\text{M}$. All the CHT-coated 5CB droplets transit to the radial configuration when the concentration of C₁₂TAB reaches to $270 \mu\text{M}$. The transition curves shift to left with the increase of n . The concentration of C_nTAB required to induce 100% of the transition drops from $\sim 270 \mu\text{M}$ to $\sim 75 \mu\text{M}$ when the chain length of C_nTAB increases from $n = 12$ to $n = 18$. These concentrations are significantly lower than the critical micelle concentration of C₁₂TAB (15mM) and C₁₈TAB (0.9 mM), suggesting that there is no aggregation for SC₁₂S and SC₁₈S, which were used in our experiments. **Figure 4(b)** shows the transition curves of negatively charged PSS-modified 5CB droplets as a function of C_nTAB concentrations. The adsorption of C₁₂TAB on the PSS-modified 5CB droplets was confirmed by the decrease of the ζ -potentials of CHT-coated 5CB droplets from -43 mV to -11 mV after 30 min incubation with the positive charged C₁₂TAB. The transition curves are shifted leftwards with the increase of n . It is clear from **Figure 4(c)** that the concentration of C_nTAB required to induce the 100% transition of PSS-coated 5CB droplets is much lower than that of the CHT-coated 5CB droplets. For $n = 18$, the 100% transition of PSS-coated 5CB droplets takes place at the C₁₈TAB concentration of $\sim 10 \mu\text{M}$, while is lower than the concentration of C₁₈TAB required to induce the 100% transition of CHT-coated 5CB droplets ($\sim 75 \mu\text{M}$). Again, the differences are significantly enlarged with the decrease of n .

Furthermore, we study the interaction of nonionic C_nE₄ with positively charged CHT and negatively charged PSS-coated 5CB droplets. For $n = 12$ or 14 , there are only slightly shifts observed in the transition curves between positively charged CHT-coated 5CB droplets and negatively charged PSS-coated 5CB droplets (**Figure 5(a)**). The concentration of SC₁₄S required to induce the 100% transition of CHT- and PSS-coated 5CB droplets is near the same. While the concentration of SC₁₂S required inducing the 100% transition of PSS-coated 5CB droplets is slightly larger than that of CHT-coated 5CB droplets (**Figure 5(b)**). This result suggests that the charged polyelectrolyte-coating has no significantly effect on the interaction between the 5CB droplet cores and nonionic C_nE₄. Finally, we compare the transition curves of positively charged CHT-coated 5CB droplets for anionic C₁₂TAB, ionic SC₁₂S, and nonionic C₁₂E₄ (**Figure 6(a)**). The concentration of nonionic C₁₂E₄ required to induce the 100% transition of PSS-coated 5CB droplets is near the same as cationic C₁₂TAB, but significantly lower than anionic SC₁₂S. Similar results are observed for anionic C₁₄TAB, ionic SC₁₄S, and nonionic C₁₄E₄ (**Figure 6(b)**).

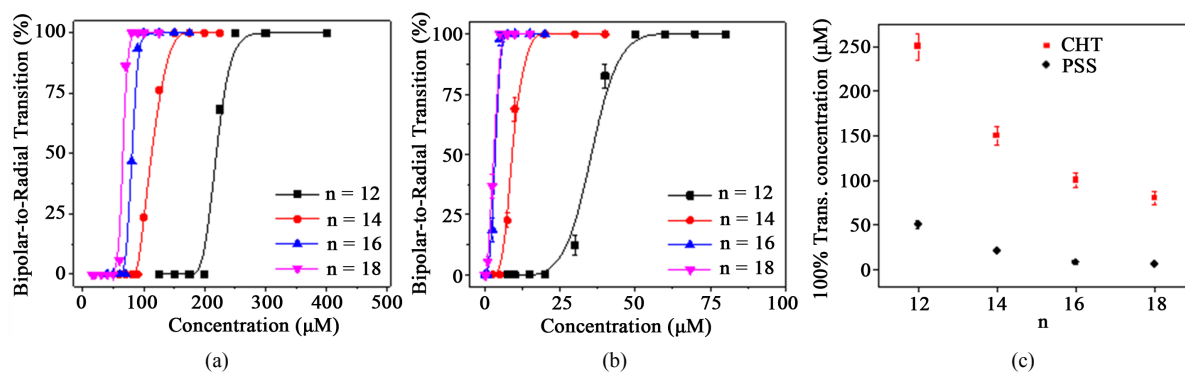


Figure 4. (a) The bipolar-to-radial transition percentage of CHT-coated 5CB droplets as a function of C_nTAB concentrations; (b) The bipolar-to-radial transition percentage of PSS-coated 5CB droplets as a function of C_nTAB concentrations; (c) C_nTAB concentration required to induce the 100% transition of CHT and PSS-coated 5CB droplets as a function of n . The data points shown in 4(a) and 4(b) were obtained from the statistical results of 100 droplets from each sample.

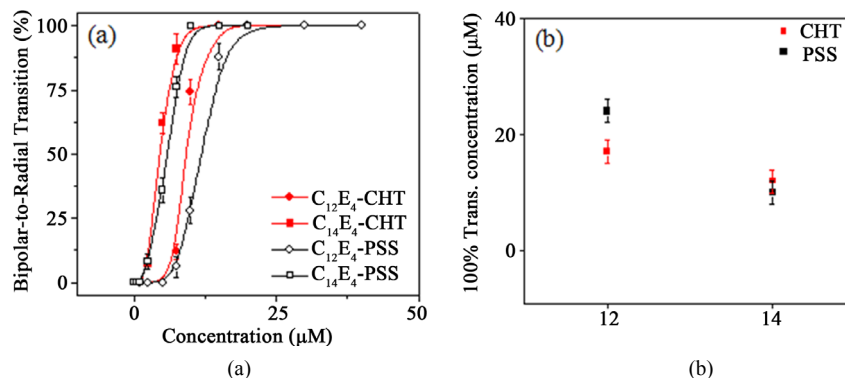


Figure 5. (a) The bipolar-to-radial transition percentage of CHT- and PSS-coated 5CB droplets as a function of C_nE_4 concentrations; (b) C_nE_4 concentration required to induce the 100% transition of CHT and PSS-coated 5CB droplets as a function of n . The data points shown in 4a and 4b were obtained from the statistical results of 100 droplets from each sample.

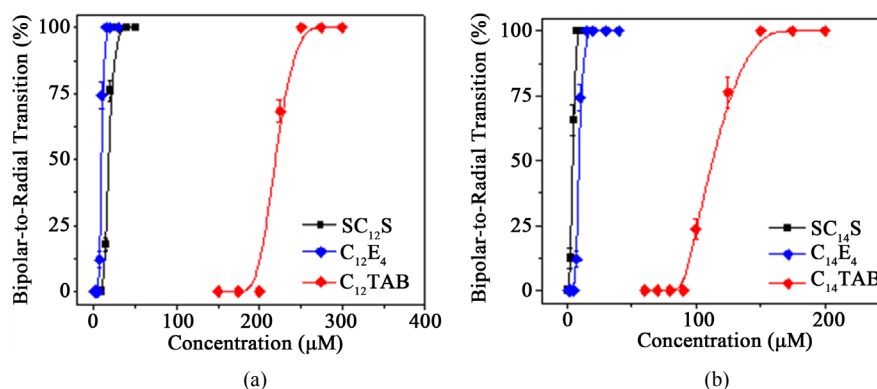


Figure 6. (a) The bipolar-to-radial transition percentage of CHT-coated 5CB droplets as a function of $SC_{12}S$, $C_{12}TAB$, and $C_{12}E_4$ concentrations; (b) The bipolar-to-radial transition percentage of CHT-coated 5CB droplets as a function of $SC_{14}S$, $C_{14}TAB$, and $C_{14}E_4$ concentrations.

4. Conclusion

We have shown that the surfactant-induced configuration transition of charged polyelectrolyte-coated 5CB droplets is affected by the electrostatic interaction between charged surfactants and charged polyelectrolyte coatings. The charged polyelectrolyte coating causes the increase of the concentration of surfactants with the same charge, which is required to induce the bipolar-to-radial transition of the LC droplet cores. The effect of charged polyelectrolyte coatings is significantly enlarged with the decrease of surfactant chain lengths. Our results suggest the possibility of engineering polyelectrolyte coatings to tune the interaction of LC droplet cores with surfactants, which is critical towards designing LC droplet based sensors.

Acknowledgements

This work was supported by USA National Science Foundation (CBET-1264355).

References

- [1] Volovik, G.E. and Lavrentovich, O.D. (1983) Topological Dynamics of Defects: Boojums in Nematic Drops. *Journal of Experimental and Theoretical Physics*, **58**, 1159-1167.
- [2] Hsu, P., Poulin, P. and Weitz, D.A. (1998) Rotational Diffusion of Monodisperse Liquid Crystal Droplets. *Journal of Colloid and Interface Science*, **200**, 182-184. <http://dx.doi.org/10.1006/jcis.1997.5223>
- [3] Juodkazis, S., Shikata, M., Takahashi, T., Matsuo, S. and Misawa, H. (1999) Fast Optical Switching by a Laser Mani-

- ulated Microdroplet of Liquid Crystal. *Applied Physics Letters*, **74**, 3627-3629. <http://dx.doi.org/10.1063/1.123203>
- [4] Wood, T.A., Gleeson, H.F., Dickinson, M.R. and Wright, A.J. (2004) Mechanisms of Optical Angular Momentum Transfer to Nematic Liquid Crystalline Droplets. *Applied Physics Letters*, **84**, 4292-4294. <http://dx.doi.org/10.1063/1.1753067>
- [5] Brasselet, E., Murazawa, N., Misawa, H. and Juodkakis, S. (2009) Optical Vortices from Liquid Crystal Droplets. *Physical Review Letters*, **103**, 103903. <http://dx.doi.org/10.1103/PhysRevLett.103.103903>
- [6] Miller, D.S., Wang, X. and Abbott, N.A. (2014) Design of Functional Materials Based on Liquid Crystalline Droplets. *Chemistry of Materials*, **26**, 496-506. <http://dx.doi.org/10.1021/cm4025028>
- [7] Lin, I.H., Miller, D.S., Bertics, P.J., Murphy, C.J., de Pablo, J.J. and Abbott, N.L. (2011) Endotoxin-Induced Structural Transformations in Liquid Crystalline Droplets. *Science*, **332**, 1297-1300. <http://dx.doi.org/10.1126/science.1195639>
- [8] Umbanhowar, P.B., Prasad, V. and Weitz, D.A. (2000) Monodisperse Emulsion Generation via Drop Break off in a Coflowing Stream. *Langmuir*, **16**, 347-351. <http://dx.doi.org/10.1021/la990101e>
- [9] Tixier, T., Heppenstall-Butler, M., Terentjev, E.M., Tixier, T., Heppenstall-Butler, M. and Terentjev, E.M. (2006) Spontaneous Size Selection in Cholesteric and Nematic Emulsions. *Langmuir*, **22**, 2365-2370. <http://dx.doi.org/10.1021/la0531953>
- [10] Tjijto, E., Cadwell, K.D., Quinn, J.F., Johnston, A.P.R., Caruso, F. and Abbott, N.L. (2006) Tailoring the Interfaces between Nematic Liquid Crystal Emulsions and Aqueous Phases via Layer-by-Layer Assembly. *Nano Letters*, **6**, 2243-2248. <http://dx.doi.org/10.1021/nl061604p>
- [11] Simon, K.A., Sejwal, P., Gerecht, R.B. and Luk, Y.-Y. (2007) Water-in-Water Emulsions Stabilized by Non-Amphiphilic Interactions: Polymer-Dispersed Lyotropic Liquid Crystals. *Langmuir*, **23**, 1453-1458. <http://dx.doi.org/10.1021/la062203s>
- [12] Kinsinger, M.L., Buck, M.E., Abbott, N.L. and Lynn, D.M. (2010) Immobilization of Polymer-Decorated Liquid Crystal Droplets on Chemically Tailored Surfaces. *Langmuir*, **26**, 10234-10242. <http://dx.doi.org/10.1021/la100376u>
- [13] Zou, J., Bera, T., Davis, A.A., Liang, W. and Fang, J.Y. (2011) Director Configuration Transitions of Polyelectrolyte Coated Liquid-Crystal Droplets. *The Journal of Physical Chemistry B*, **115**, 8970-8974. <http://dx.doi.org/10.1021/jp201909m>
- [14] Aliño, V.A., Pang, J. and Yang, K.L. (2011) Liquid Crystal Droplets as a Hosting and Sensing Platform for Developing Immunoassays. *Langmuir*, **27**, 11784-11789. <http://dx.doi.org/10.1021/la2022215>
- [15] Khan, W., Choi, J.H., Kim, G.M. and Park, S.Y. (2011) Microfluidic Formation of pH Responsive 5CB Droplets Decorated with PAA-*b*-LCP. *Lab on a Chip*, **11**, 3493-3498. <http://dx.doi.org/10.1039/c1lc20402e>
- [16] Bera, T. and Fang, J.Y. (2012) Polyelectrolyte-Coated Liquid Crystal Droplets for Detecting Charged Macromolecules. *Journal of Materials Chemistry*, **22**, 6807-6812. <http://dx.doi.org/10.1039/C2JM00038E>
- [17] Aliño, V.J., Sim, P.H., Choy, W.T., Fraser, A. and Yang, K.Y. (2012) Detecting Proteins in Microfluidic Channels Decorated with Liquid Crystal Sensing Dots. *Langmuir*, **28**, 17571-17577. <http://dx.doi.org/10.1021/la303213h>
- [18] Manna, U., Zayas-Gonzalez, Y.M., Carlton, R.J., Caruso, F., Abbott, N.L. and Lynn, D.M. (2013) Liquid Crystal Chemical Sensors That Cells Can Wear. *Angewandte Chemie International Edition*, **52**, 14011-14015. <http://dx.doi.org/10.1002/anie.201306630>
- [19] Kim, J., Khan, M. and Park, S.Y. (2013) Glucose Sensor Using Liquid-Crystal Droplets Made by Microfluidics. *ACS Applied Materials Interfaces*, **5**, 13135-13139. <http://dx.doi.org/10.1021/am404174n>
- [20] Bera, T. and Fang, J.Y. (2014) Protein-Induced Configuration Transition of Polyelectrolyte-Modified Liquid Crystal Droplets. *The Journal of Physical Chemistry B*, **118**, 4970-4977. <http://dx.doi.org/10.1021/jp501587h>
- [21] Murazawa, N., Juodkakis, S. and Misawa, H. (2005) Characterization of Bipolar and Radial Nematic Liquid Crystal Droplets Using Laser-Tweezers. *Journal of Physics D: Applied Physics*, **38**, 2923-2927. <http://dx.doi.org/10.1088/0022-3727/38/16/027>
- [22] Bera, T. and Fang, J.Y. (2013) Optical Detection of Lithocholic Acid with Liquid Crystal Emulsions. *Langmuir*, **29**, 387-392. <http://dx.doi.org/10.1021/la303771t>
- [23] Malone, S.M. and Schwartz, D.K. (2008) Polar and Azimuthal Alignment of a Nematic Liquid Crystal by Alkylsilane Self-Assembled Monolayers: Effects of Chain-Length and Mechanical Rubbing. *Langmuir*, **24**, 9790-9794. <http://dx.doi.org/10.1021/la801322x>
- [24] Price, A.D. and Schwartz, D.K. (2007) Fatty-Acid Monolayers at the Nematic/Water Interface: Phases and Liquid-Crystal Alignment. *The Journal of Physical Chemistry B*, **111**, 1007-1015. <http://dx.doi.org/10.1021/jp066228b>
- [25] Brake, J.M. and Abbott, N.L. (2002) An Experimental System for Imaging the Reversible Adsorption of Amphiphiles at Aqueous-Liquid Crystal Interfaces. *Langmuir*, **18**, 6101-6109. <http://dx.doi.org/10.1021/la011746t>
- [26] Fang, J.Y., Gehlert, U., Shashidhar, R. and Knobler, C.M. (1999) Imaging the Azimuthal Tilt Order in Monolayers by Liquid Crystal Optical Amplification. *Langmuir*, **15**, 297-299. <http://dx.doi.org/10.1021/la9812929>

Scientific Research Publishing (SCIRP) is one of the largest Open Access journal publishers. It is currently publishing more than 200 open access, online, peer-reviewed journals covering a wide range of academic disciplines. SCIRP serves the worldwide academic communities and contributes to the progress and application of science with its publication.

Other selected journals from SCIRP are listed as below. Submit your manuscript to us via either submit@scirp.org or [Online Submission Portal](#).

